



In situ pre-concentration and voltammetric determination of trace lead and cadmium by a novel ionic liquid mediated hollow fiber-graphite electrode and design of experiments via Taguchi method



Zarrin Es'haghi ^{a,*}, Tahereh Heidari ^b, Ehsan Mazloomi ^a

^a Department of Chemistry, Payame Noor University, Tehran 19395-4697, IRAN

^b Department of Chemistry, Faculty of Sciences, Ferdowsi University of Mashhad, Mashhad, Iran

ARTICLE INFO

Article history:

Received 2 July 2014

Received in revised form 20 September 2014

Accepted 24 September 2014

Available online 28 September 2014

Keywords:

Pb(II)

Cd(II)

Hollow fiber-graphite supported
nanomagnetite/ionic liquid electrode
Differential pulse voltammetry
Taguchi method

ABSTRACT

In this research a single-use voltammetry sensor, incorporating a three electrodes configuration was developed, using ionic liquid mediated hollow fiber-graphite supported nanomagnetite working electrode. These electrodes coupled with differential pulse voltammetry (DPV) provided a screening tool for in-situ pre-concentration and determination of trace levels of Pb(II) and Cd(II). In this design, a two-centimeter piece of porous polypropylene hollow fiber membrane was impregnated with homogeneous mixture of nanomagnetic particles/ionic liquid (1-butyl-3-methylimidazolium hexafluorophosphate), and a graphite rod was located inside the fiber lumen. In this sensor, synthesized nanoparticles such as zero-valent Iron (ZVI), nanomagnetite (NM) and magnetic hollow spheres (MHS), dispersed in the ionic liquid, were used for one-step simultaneous purification, pre-concentration and trapping of pb(II) and Cd(II) ions from water samples. The Taguchi method was applied as an experimental design to determine optimum conditions for lead and cadmium ions removal. The experiments were designed, in two steps, according to Taguchi's method, OA₁₆ L₁₈ (2¹ × 3⁵) and OA₁₆ L₁₆ (2¹ × 4³) orthogonal were arrayed to the optimize experimental runs. Various affective parameters were investigated. The effect of all the input parameters on the output responses was analyzed using analysis of variance (ANOVA). The results revealed that the metal removal was influenced primarily by the amount of nanoparticle (52.18%) and agitation rate (19.71%). The extraction time (8.97%) and mercury acetate concentration in the electrolyte (7.6%) had little significant influence on metal removal efficiency. The performance characteristics of the developed method were evaluated by assessing response linearity and precision. The method was suitable for the quantitation of pb(II) and Cd(II) ions in the concentration range of 2–13000 ng mL⁻¹ and 0.6–6500 ng mL⁻¹ for Cd(II) and Pb(II) ions respectively. The detection limits recorded for Cd(II) and Pb(II) were 0.61 and 0.19 ng mL⁻¹ with relative standard deviation (RSD) of 4.6%, and 2.3%, respectively. Moreover, successful applications of the sensing device to real water samples were demonstrated.

© 2014 Elsevier Ltd. All rights reserved.

1. Introduction

Human activities through technological development and industrial events discharge heavy metals into the environment which has become a matter of concern over the past few decades, due to the characteristics of metals to cause contestable effects by reducing the quality of life in the environment [1–3]. From this perspective, removal of heavy metals is very important because they are non-biodegradable [4,5].

Among the available techniques for trace elements analysis electrochemical methods are very attractive in this field [6–8]. Different types of electrodes such as hanging mercury electrodes, mercury plated thin film and glassy carbon electrode were used in field experiments [8–10]. However, due to the difficulties in using the electrodes for field analysis, the development and application of single-use electrodes is widely reported [11,12]. Disposable electrodes are designed for one use and therefore have the advantages of not being affected by the problems associated with carryover of contaminants and this minimizes the damage often associated with a re-usable sensors [13].

Also, sample preparation techniques have been widely used for the pre-concentration and separation of trace metal ions in

* Corresponding author. Tel.: +98 5118691088; fax: +98 511 8683001.

E-mail address: eshaghi@pnu.ac.ir (Z. Es'haghi).

aqueous systems prior to their determination. Among the available techniques, solid phase microextraction (SPME) is one of the most interesting methods [14,15]. SPME fibers, however, are expensive and have fragile coatings and should be handled carefully. So, this study aimed to promote the SPME technique by inserting nanoparticles into the pores of polypropylene hollow fibers via an organic solvent as a solid/liquid sorbent. Hence, the idea was to have a membrane based, activated nanoparticles that acts as an analyte trap, lead in higher selectivity and enrichment, because the nanoparticles act as solid sorbents do in SPME fibers. So, the attachment of the analyte was accomplished by two different chemical approaches; non-covalent and covalent binding. Results showed significant improvement in the ordinary SPME fibers [16,17].

In the present work this μ -SLPME fiber was coupled with an electrochemical system. In this new application, the role of the background solvent is important. So the solvent would allow metal ions to penetrate into the membrane. The solvent also should be consistent with the structure of the fiber, so that would do not leave the fiber pores. Many solvents were tested and finally an ionic liquid (1-butyl-3-methylimidazolium hexafluorophosphate) was selected.

Furthermore, an electrical conductor interface was needed. The electrical contact was established via a graphite pencils that were placed inside the fiber and connected to a copper wire. In this context, the used device for this study was provided by the authors. Disposable nature of the fiber (although this fiber can be reused multiple times) eliminates the risk of carry over, too. Easy preparation process, low background current, high sensitivity, stability, and small loading of nanoparticle using this combination can create new potentials and applications for fabricating robust sensors for many important species.

According to the conditions listed above, the present study aimed to couple this innovative nanoparticle assisted hollow fiber graphite sensor with an electrochemical system. So that the fiber would play the role of a solid/liquid microextraction device and simultaneously, serve as the working electrode or a pseudo electrochemical sensor for Pb(II) and Cd(II) metal ions.

2. Experimental

2.1. Chemicals and Materials

The Accurel Q 3/2 polypropylene hollow fiber membrane which was used here was obtained from Membrana (Wuppertal, Germany). The wall thickness of the fiber was 200 μm , the inner diameter was 600 μm , and the pore size was 0.2 μm .

Some of nanoparticles such as zero-valent iron (ZVI), nano-magnetic Fe_3O_4 (NM), magnetic hollow spheres (MHS) were synthesized in the authors' laboratory. Analytical $\text{FeCl}_3 \cdot 6\text{H}_2\text{O}$, $\text{FeCl}_2 \cdot 4\text{H}_2\text{O}$, $\text{FeSO}_4 \cdot 7\text{H}_2\text{O}$, $\text{Hg}(\text{CH}_3\text{COO})_2$, NaClO_4 , NH_3 , sodium borohydride (NaBH_4), Ethylenediaminetetraacetic acid (EDTA), n-hexane, surfactants; Span-80 and Tween-80, all were purchased from Merck (Darmstadt, Germany). Ionic liquid, 1-butyl-2,3-Dimethylimidazolium hexafluorophosphate [BDMIM][PF6] was provided by Sigma-Aldrich company (St. Louis, USA). All chemicals which were used were of at least analytical-reagent grade. Triple time distilled and de-ionized water was used throughout.

Stock solutions of 100 $\text{mg}\cdot\text{L}^{-1}$ of each Cd(II), Pb(II) ions were prepared by dissolving appropriate amount of cadmium nitrate and copper nitrate (all purchased from Merck) in de-ionized (DI) water and diluted to 100 mL volumetric flask. Working standard solutions were obtained by appropriate dilution of the stock standard solution.

2.2. Instrumentation

All the voltammetric measurements were performed by trace analyzer, Metrohm Model 797 VA computerace (Switzerland), comprising three electrode arrangements such as Ag/AgCl (saturated KCl) as a reference electrode and platinum wire as an auxiliary/counter electrode and the home-made hollow fiber graphite electrode (HF-GE) as a working electrode. The voltammograms of Cd(II), Pb(II) ions were obtained by DPV mode. The volume of the solution introduced in the voltammetric cell was 15.0 mL. The solutions were de-aerated by ultrapure N_2 gas for 300 s. The voltammetric experimental variables such as; scan rate of the electrode potential, voltage step, voltage step time, equilibrium time, deposition time and stirring speed of the solution were optimized. The deposition time study was carried out from 0 to 3000 s as the on-line pre-concentration time of analyte.

Effect of deposition potential on peak currents of Cd(II), Pb(II) ions was tested between -0.85 to -0.41 V. The other DPV optimal conditions were as follows; equilibration time 10 s, pulse amplitude 0.09003 V, pulse time 0.01 s, sweep rate 19.8 $\text{mV}\cdot\text{s}^{-1}$, voltage step 0.007935 V and voltage step time 0.4 s and the operational mode was, differential pulse voltammetry.

Nanoparticles morphology, size distribution and structure were characterized by direct light scattering (DLS, Zetaplus, Brookhaven 9000 instruments), SEM (JEOL JEM2000, Nikon, Japan) and FT-IR spectroscopy (ATI Mattson, Genesis series FT-IR).

2.3. Synthesis of nanoparticles

2.3.1. Synthesis of nano zero-valent iron (ZVI)

This synthesis was stabilized by disodium salt of EDTA (Sample 1). As the zero-valent irons are very active materials in the presence of air and high potential to agglomeration, electrochemical sensor for metal ions ZVI was synthesized by EDTA because chelating agents such as EDTA can be assisted to stabilization of the ZVI [18]. The ZVI was prepared with a chemical reduction procedure. At first 75.0 mL of EDTA solution (0.15 M) was added to 100.0 mL of FeCl_3 (0.3 M) solution which was vigorously mixed with magnetic stirrer in the flask reactor. Then 100 mL NaBH_4 (1.5 M) was added to this mixture drop-wise at room temperature under a N_2 atmosphere. Sweep rate of reduction was 20 $\text{mL}\cdot\text{min}^{-1}$ and molar ratio $\text{Fe}_3^+/\text{BH}_4^-$ was 1:5 because these conditions have provided maximum surface area ($\text{m}^2\cdot\text{g}^{-1}$) and minimum particle size [19]. After adding the whole reagents, color of the solution changed from brown to dark-green and the black nano particles (NPs) were formed (pH 8.5). Finally, black products were rinsed by oxygen-free deionized water three times to remove residual impurities and then vacuum-dried.

2.3.2. Synthesis of the magnetic hollow spheres (MHS) iron nanoparticles

Magnetic hollow spheres iron nanoparticles were prepared according to the previously published method [20]. Briefly, an aqueous solution of $\text{NH}_3\cdot\text{H}_2\text{O}$ 25.00 wt % (10 mL) as precipitant was dispersed in oil phase containing n-hexane (20 mL), span-80 (1.20 g) and Tween-80 (0.90 g). After 10 min sonication, the aqueous solution containing 3.85 g of $\text{FeCl}_3\cdot\text{H}_2\text{O}$ and 2.00 g of FeSO_4 (70 mL) was added to the previous mixture. This method led to hollow structure with good spherical morphology. The reaction system maintained for 12 h at 20 °C under mechanical stirring at nitrogen atmosphere. The product was washed with deionized water several times and dried in room temperature.

2.3.3. Synthesis of Nano Magnetic Fe_3O_4 (NM)

Before the addition of any salt, 200 mL of water which was used in the experiments was bubbled with nitrogen for 15 min to remove dissolved oxygen. Then, 5.12 g ferric chloride hexahydrate

($\text{FeCl}_3 \cdot 6\text{H}_2\text{O}$) and 2.00 g of ferrous chloride tetra-hydrate ($\text{FeCl}_2 \cdot 4\text{H}_2\text{O}$) were dissolved in water. Subsequently, the solution was heated slowly until temperature reached to 80°C then under nitrogen atmosphere and stirring (600 rpm), ammonia solution (1.5 M) were added drop-wise until pH passed away from 8. Then the temperature, stirring rate, and nitrogen bubbling conditions were maintained for 2 h, finally the generated black Fe_3O_4 nanoparticles were collected by an external magnet, washed with water to neutral pH and then dried in the air atmosphere [21].

2.4. Characterization of the synthesized nanoparticles

To determine the physical characteristics of magnetic nanoparticles, particle size and size distribution were analyzed. Direct light scattering analysis was used to determine the size and the

size distribution. Particle size distributions were shown in Fig. 1. Scanning electron microscopy (SEM) analysis was performed to observe morphology and size of the nanoparticles. FT-IR analysis was used to verify the presence of the magnetic nanoparticles.

The nanoparticles with smooth surfaces and moderately uniform size distributions were obtained. The mean size and the size distribution of prepared particles measured by laser scattering showed; NM: 64.31 ± 5 , ZVI: 194.18 ± 5 , MHS: 534.94 ± 5 nm with acceptable size distributions.

2.5. Fabrication of the hollow fiber graphite electrode (HF-GE)

First, a polypropylene hollow fiber was cut into segments with a length of 2.0 cm. The fiber segments were cleaned with acetone to remove impurities and directly dried in air. 1.7 cm of a cleaned

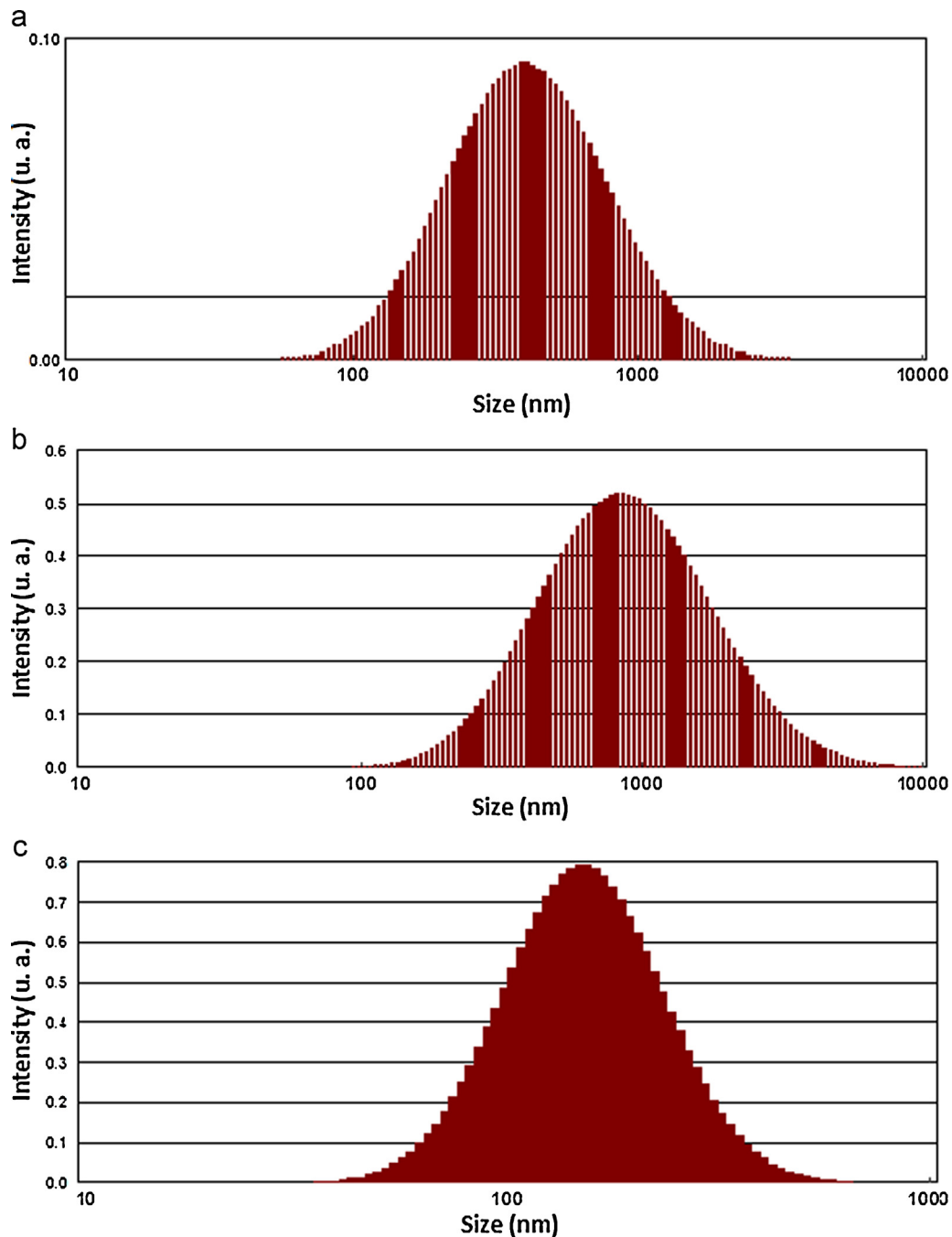


Fig. 1. Size distribution of the three synthesized structures of iron. (a) zero-valent Iron (ZVI), (b) magnetic hollow spheres (MHS), (c) Fe_3O_4 (NM).

graphite pencils rod (O.D. 0.7 mm and 2.5 cm length) was inserted carefully into the fiber segment. In preliminary tests, before use the graphite electrode was modified using the mercury acetate solution. Each mercury coated graphite electrode was pretreated by applying -1.1 volt for 300 Sec to convert the mercury acetate to Hg. Thereby a mercury film was produced on the graphite surface to provide a conductive support for a thin mercury film to produce an electrode. Generally, such graphite supported mercury film is useful as an electrode, particularly for electroanalytical techniques such as differential pulse voltammetry. However, due to the presence of nanoparticles the effect of mercury film had not a dramatic impact.

The free end of hollow fiber was closed by heating. In the second stage, 5.0 mL ionic liquid was added to the conical tube and appropriate amount of optimum magnetic nanoparticles (30 mg) were dispersed in the ionic liquid. The kind of nanoparticles such

as ZVI, MHS, and NM were already been optimized. Eventually, the fabricated HF-EG was directly put on this mixture and sonicated before the analysis (10 min). Fig. 2 shows the scheme of HF-GE in ionic liquid and SEM images of fiber with detail. The hollow fiber was taken out from the conical tube and washed twice with 1–2 mL deionized water then transferred into voltammetric cell. Each HF-GE was used only once to avoid any memory effect.

3. Results and discussion

All experiments carried out in this study were repeated at least three times. The data represented the mean value of three measurements. HCl and mercury acetate with optimal concentrations were chosen as the supporting electrolyte for lead and cadmium ions analysis on the basis of sensitivity as well as the need for chloride ions in the test solution for stabilizing the

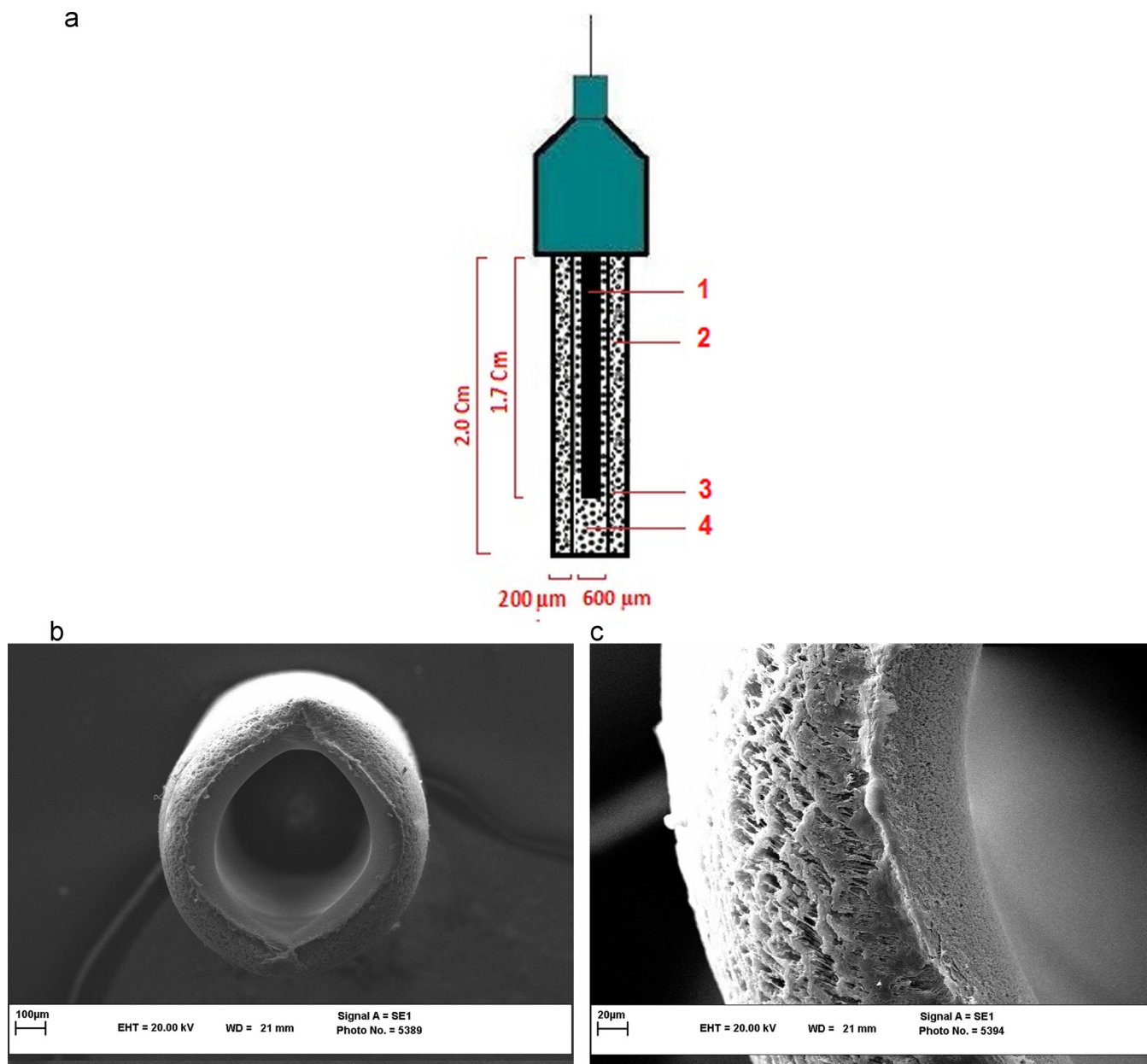


Fig. 2. HF-GE structure. (a) Electrode scheme; (1) Graphite rod: 1.7 Cm, (2) mixture of ionic liquid and nM with ratio of 30 mg nM per 5 mL IL, (3) Hollow fiber pores: 0.2 μ m, (4) Lumen of the hollow fiber. (b) Scanning electron microscopy (SEM) of polypropylene hollow fiber. (c) SEM image of polypropylene hollow fiber impregnated with homogenised mixture of nM and ionic liquid.

Table 1
Factors and their levels for design of experiments in the first step.

Parameter	Level		
	1	2	3
(A) NP amount (g)	0.003	0.007	
(B) Type of NP	ZVI	MHS	nM
(C) Hg (II) concentration (ppm)	30	50	70
(D) HCl concentration (M)	0.125	0.2	0.275
(E) Time (s)	0	900	1800
(F) Stirring speed (rpm)	200	600	1000

Table 2
Taguchi L18 ($2^1 \times 3^4$) orthogonal array and results in term of peak current

Trial No.	Factor						Current (mA) $\times 10^{-2}$		
	A	B	C	D	E	F	Cd	Pb	sum
1	1	1	1	1	1	1	11	7.59	18.59
2	1	1	2	2	2	2	13.5	9.94	23.44
3	1	1	3	3	3	3	10.7	6.65	17.35
4	1	2	1	1	2	2	4.73	8.06	12.79
5	1	2	2	2	3	3	9.07	9.88	18.95
6	1	2	3	3	1	1	9.55	7.41	16.96
7	1	3	1	2	1	3	9.96	14.5	24.46
8	1	3	2	3	2	1	11.5	9.36	20.86
9	1	3	3	1	3	2	13.1	11.1	24.2
10	2	1	1	3	3	2	12.3	11.1	23.4
11	2	1	2	1	1	3	4.82	7.9	12.72
12	2	1	3	2	2	1	9.02	7.68	16.7
13	2	2	1	2	3	1	4.44	6.83	11.27
14	2	2	2	3	1	2	2.31	4.26	6.57
15	2	2	3	1	2	3	4.26	5.63	9.89
16	2	3	1	3	2	3	9.79	8.67	18.46
17	2	3	2	1	3	1	13.01	11.02	24.03
18	2	3	3	2	1	2	4.13	4.85	8.98

potential of the Ag/AgCl reference electrode reference electrode. Hydrochloric acid (HCl) was used instead of potassium chloride (KCl) because HCl is normally free from metal ion impurities compared to KCl and mercury acetate was added to increase the pH of media above 2.0 for increase the sensitivity. The effect of experimental variables such as the effect of deposition potential, deposition time and the concentration dependence for each of the metal ions were investigated. In situ desorption and analysis was occurred because it simplified the experimental procedure.

3.1. Taguchi's orthogonal array (OA) experiments

In this research the Taguchi method was used to improve the productivity and sensitivity levels. Taguchi claims that noise interactions have the greatest importance in attaining a design that is robust to noise factor variation. The Taguchi approach provides more interactive information than the typical fractional factorial designs.

Table 3
ANOVA results for experimental responses in the OA₁₆ L₁₈ ($2^1 \times 3^4$).

Source	DOF	SS	Adj SS	Variance	F-ratio	P	PC(%)
A	1	115.419	115.419	115.419	60.45	0.016	20.81
B	2	185.686	185.686	92.843	48.62	0.02	33.47
C	2	21.304	31.345	15.672	8.21	0.109	3.84
D	2	0.247	0.247	0.123	0.06	0.939	0.04
E	2	79.955	79.955	39.977	20.94	0.046	14.41
F	2	7.269	85.680	42.840	22.44	0.043	1.31
A \times B	2	19.344	19.344	9.672	5.07	0.165	3.49
A \times D	2	121.684	121.684	60.842	31.86	0.03	21.94
Error	2	3.819	3.819	1.909			0.69
Total	17	554.727					100

DOF: Degree of freedom, SS: Sum of squares, PC: Percent contribution
F critical (1,2;0.05)= 18.51, F critical (2,2;0.05)=19.00.

After the calculation, experimental results were analyzed with the help of performance statistics and analysis of variance (ANOVA). Following is the selection levels of process parameters. Finally, optimal process parameters were verified through the confirmation experiment.

In this work, Taguchi's OA analysis was used within two steps to produce the best parameters for the optimum design process, with the least number of experiments. The peak current of lead and cadmium were considered as the experimental response.

In the first step, the effect of six important factors including; sorbent dosage in the ionic liquid, type of nanostructures of iron, concentration of mercury acetate and hydrochloric acid in voltammetric cell, extraction time and stirring speed were studied using Taguchi's method. In all cases it should be noted that each reported response is the average of three measurements. The used level setting values of the main factors (A–F) and the OA₁₆ L₁₈($2^1 \times 3^5$) matrix employed to assign the considered factors are shown in Tables 1 and 2, respectively.

After the first step, nanomagnetite (Fe₃O₄) was selected as the best nanostructure of iron that can help the extraction process and the other parameters were optimized, accordingly. Also since in the first step the concentration of the HCl was not detected among the main factors, this factor kept constant in the optimum level. Therefore, in the second step, four parameters were considered.

The Taguchi L₁₆ ($2^1 \times 4^3$), orthogonal mixed factorial array (two levels for amount of nano Fe₃O₄ and four levels for Hg (II) concentration, extraction time and stirring speed parameters) was selected in order to find out the optimum levels of parameters. Experimental parameter and their levels are shown in Table 3 and the OA₁₆ L₁₆ ($2^1 \times 4^3$) experimental design is reported in Table 4. In doing this, Minitab® 16 Statistical Software was used. The flow chart of experimental design is shown in Fig. 3.

3.1.1. Study of the HF-GE method variables in step one

To take the optimum advantages of the procedure, various experimental parameters must be studied to obtain an optimized scheme. These parameters were optimized in the present research by an orthogonal mixed factorial array, five-factor tree-levels and one-factor two-levels and the experimental data were evaluated using Minitab 16 Software. The mean values of the levels of each factor revealed how the extraction efficiency changes when the level of that factor changes.

3.1.1.1. Effect of the type of nanoparticle. According to the results listed in Table 3, it is known that nanomagnetite (Fe₃O₄, nM) has the greatest impact and the iron hollow sphere (MHS) has the least influence on the extraction process. These results can be attributed to the size of nanoparticles. As the size of the particles would be smaller, surface area-to-ionic liquid volume ratio would be greater. Therefore, smaller particles can efficiently adsorb analytes and have more interaction with them. According to Table 3, analysis of

Table 4
Factors and their levels for design of experiments.

Parameter	Level			
	1	2	3	4
(A) Extraction time (s)	1200	1800	2400	3000
(B) Stirring speed (rpm)	0	200	400	600
(C) Hg (II) concentration (ppm)	10	30	50	70
(D) Nano magnetic (g)	0.001	0.003		

DOF: degree of freedom, SS: sum of squares, PC: percent contribution
F critical (1, 5; 0.05) =6.608, F critical (3, 5; 0.05) =5.409.

variance, the high contribution of this factor (% 47/33), indicating the importance of it. Results of Taguchi L16 ($2^1 \times 4^3$) orthogonal array and the ANOVA results are depicted in Tables 5 and 6.

3.1.1.2. Influence of amount of nanosorbent. At this point, for all three types of magnetic nanoparticles, two levels of 0.003 and 0.007 g were considered. While ionic liquid volume was constant

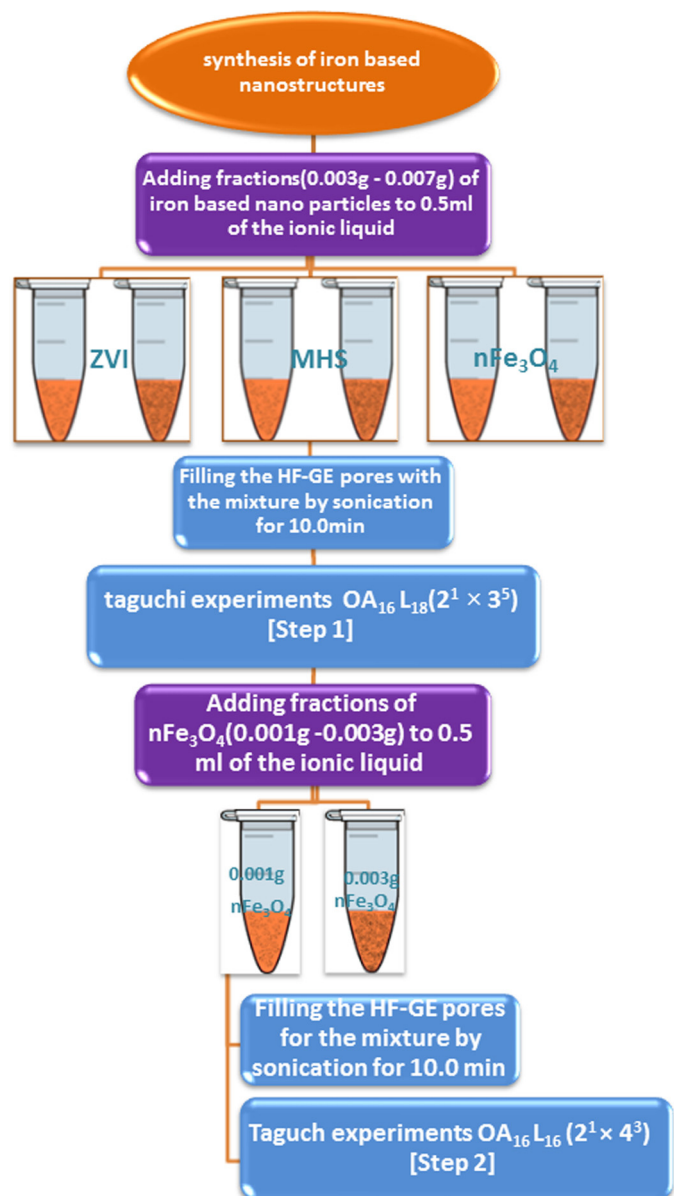


Fig. 3. Two steps experimental design of Taguchi orthogonal array.

Table 5
Taguchi L16 ($2^1 \times 4^3$) orthogonal array and results of peak current

Trial No.	Factor				Current (mA) $\times 10^{-2}$		
	A	B	C	D	Cd	Pb	sum
1	1	1	1	1	7.16	11.21	18.37
2	1	2	2	1	10.85	11.26	22.11
3	1	3	3	2	10.79	7.9	18.7
4	1	4	4	2	10.91	10.98	21.89
5	2	1	2	2	11.1	11.4	22.5
6	2	2	1	2	11.92	12.05	23.97
7	2	3	4	1	8.95	8.1	16.96
8	2	4	3	1	9.92	8.79	18.71
9	3	1	3	1	9.21	7.55	16.76
10	3	2	4	1	10.1	7.46	17.56
11	3	3	1	2	12.3	10.44	22.73
12	3	4	2	2	11.8	10.91	22.7
13	4	1	4	2	10.92	7.6	18.5
14	4	2	3	2	12.4	11.01	23.41
15	4	3	2	1	8.23	7.32	15.55
16	4	4	1	1	8.83	7.3	16.13

and equal to 0.50 mL. Therefore, six conical tubes within 0.5 mL ionic liquids containing iron nanoparticles with the above values were prepared. As well as the electrodes were placed in the tubes for ten minutes under ultrasound. This led to fine dispersion of magnetic nanoparticles in the ionic liquid and good penetration into the fiber pores. Fig. 4 has shown interaction between type and amount of nanoparticles according means of responses for two analytes, and indicated that low level, ie, 0.003 g, provided better results. These results can imply that increasing the amount of nanoparticles, decreases the ionic liquid volume, thus the connection between the analytes and the ionic liquid and makes deliver them to the electrode surface difficult.

3.1.1.3. Effect of the other parameters. In this study, mixture of mercury acetate and hydrochloric acid was used as supporting electrolyte. As it is shown in Table 3, low contributions of 3.84% and 0.04% for mercury acetate and HCl, are all indicative of the fact that these factors were not the influential factors. Extraction time is an important factor in the solid phase microextraction process and must be optimized.

The electrochemical method are based on mass transport through the boundary layers, such as

pre-equilibrium SPME. Based on the results, from 0.0 to 1800.0 seconds, as the length of electrode stays in the cell was higher; response to analytes was more associated with higher currents along with a steep slope. During this time, analytes had the opportunity to accumulate into the hollow fiber pores. Then, by applying a cathodic potential, analytes that were concentrated into hollow fiber, on the graphite surface was reduced. But due to steep slope of the curve, further investigation was needed about the time to reach equilibrium.

In the extraction, stirring speed has a direct effect on increasing the contact area between two phases and causes the mass transfer are well done. So, for study the effect of stirring speed on the

Table 6
ANOVA results for experimental responses in the OA₁₆ L₁₆ ($2^1 \times 4^3$)

Source	DOF	SS	Adj SS	Variance	F-ratio	P	PC(%)
A	3	2.779	2.779	0.9262	1.3	0.372	8.97
B	3	6.108	6.108	2.0358	2.85	0.145	19.71
C	3	2.356	2.356	0.7853	1.1	0.431	7.6
D	1	16.17	16.17	16.1705	22.61	0.005	52.18
Error	5	3.576	3.576	0.7152			11.54
total	15	30.988					100

DOF: degree of freedom, SS: sum of squares, PC: percent contribution
F critical (1,5;0.05) =6.608, F critical (3,5;0.05) =5.409.

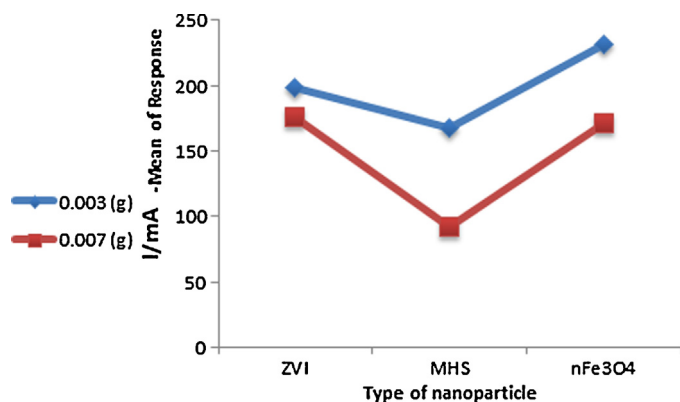


Fig. 4. Relationship between type and amount of nanoparticles based on value of Mean of Response for two analytes.

Table 7
Optimized factors of the method

Number of factors	Factor	1	2	Level 3	4	5	Selected level
1	Type of nano structure	ZVI	MHS	nFe ₃ O ₄			nFe ₃ O ₄
2	Amount of nano sorbent (g)	0.001	0.003	0.007			0.003
3	Hg(II) Conc. (mg L ⁻¹)	10	30	50	70		30
4	HCl Conc. (M)	0.125	0.2	0.275			0.125
5	Stirring rate (rpm)	0	200	400	600	1000	200
6	Extraction time (s)	0	900	1800	2400	3000	1800

extraction, three different speeds of 200, 600 and 1000 rpm were selected. The results showed that the extraction efficiency has highest value at the lowest stirring speed. Since higher speeds cause the air bubbles around the hollow fiber. According to Table 3, this factor is also an influential factor and needs further investigation.

3.1.2. HF-GE method evaluation in the second step

In order to make more accurate assessments about some important factors, in a further step, the evaluation was conducted in terms of a mixed Taguchi L₁₆ (2¹ × 4³) orthogonal array design. The results are listed in Tables 4 to 6. The overall optimized factors are shown in Table 7.

3.2. Effect of interfering ions

The effects of common interfering ions on the extraction of Cd (II) and Pb(II) by HF-GE extraction method were investigated. In these experiments, mixed solutions of 0.3 mg.L⁻¹ Cd(II) and 0.015 mg.L⁻¹ Pb(II) containing the interfering ions were treated. The results can be seen in Table 8.

Table 9
Determination of the Pb(II) and Cd(II) ions in various water sample.

Sample	Spiked level (ng ml ⁻¹)		Found (ng ml ⁻¹)		Recovery (%)	
	Cd ²⁺	Pb ²⁺	Cd ²⁺	Pb ²⁺	Cd ²⁺	Pb ²⁺
Tap water	0.00	0.00	ND	1.65±0.56		
	30.00	15.00	28.66±0.61	17.03±0.34	95.53	102.53
mineral water	0.00	0.00	ND	ND		
	30.00	15.00	28.48±0.90	14.42±0.65	94.93	96.13
River water 1	0.00	0.00	ND	ND		
	30.00	15.00	28.32±0.44	14.78±0.19	94.4	98.53
River water 2	0.00	0.00	3.10±0.22	2.15±0.38		
	30.00	15.00	32.56±0.66	16.68±0.87	98.2	96.86
Wastewater	0.00	0.00	291.06±2.29	143.21±1.02		
	30.00	15.00	324.26±1.98	158.71±1.18	110.67	103.33

Table 8
Tolerance of the interfering ions.

Interfering ions	Concentration (ng ml ⁻¹)		Tolerance limit of ions (ng ml ⁻¹)	
	Cd ²⁺ (30)	Pb ²⁺ (15)	Cd ²⁺	Pb ²⁺
Na ⁺ ,K ⁺ ,Ni ²⁺ ,Co ²⁺	×500	×1000	×500	×1000
	×100	×200		
	×10	×20		
Cl ²⁺	×500	×1000		×1000
	×100	×200	×100	
	×10	×20		
IO ₃ ²⁻ ,SO ₃ ²⁻ ,CO ₃ ²⁻	×500	×1000	×500	×1000
	×100	×200		
	×10	×20		

3.3. Analytical figures of merit

In the optimized conditions which were obtained after two steps experimental designed, the calibration equations are derived by regression analysis between measurements of peak current and standard concentrations of analytes. The linear equations for Cd²⁺ and Pb²⁺ are:

$$y = 3.00 \times 10^{-5} (\pm 1.20 \times 10^{-7}) x + 2 \times 10^{-6} (\pm 0.50 \times 10^{-6}) \text{ and } y = 6.00 \times 10^{-5} (\pm 2.40 \times 10^{-7}) x - 3 \times 10^{-6} (\pm 0.10 \times 10^{-7}) \text{ respectively.}$$

line was linear in the range of 2–13000 ng.mL⁻¹ and 0.6–6500 ng.mL⁻¹ with correlation coefficients 0.998 and 0.997 for cadmium and lead respectively. The limit of detection (LOD) of the new method for determination of Cd (II) and Pb (II) was studied under the optimal experimental conditions. The LODs were obtained from $C_{LOD} = (K_b S_b / m)$, where m is the slope of the calibration graph, K_b is the numerical value of 3 and S_b is the standard deviation of five replicates of the blank measurement. LODs were 0.61 and 0.19 ng. mL⁻¹ of Cd (II) and Pb (II) respectively.

Table 10
Comparison between methods of determination of Pb(II) and Cd(II) ions in real samples.

Metal ions	Date	Matrix	Extraction method	Detection	LOD(ng mL^{-1})	DLR(ng mL^{-1})	r^2	RSD%	Ref.
Cd ²⁺	2012	Tap water	Bi–SbFE ^a	SWASV ^b	0.15	1–220	0.998	0.99–4.41	[22]
Cd ²⁺	2012	Drinking, pond water and tap water	SPE	DPASV	0.01	15–70	–	2.56–5.67	[23]
Pb ²⁺		green tea, soup, fish and cockle			0.01	0.5–15	–		
Cd ²⁺	2011	Rice	HF-SPME ^a	DPASV	0.01	0.05–500	0.995	<5	[24]
Pb ²⁺					0.025	0.05–500	0.991		
Cd ²⁺	2011	Tap mineral, river, sea and lab water	HMDE ^a	DPASV	0.02	0.8–70	0.999	1.27–1.38	[25]
		tomato, rice, tea and spinach							
Cd ²⁺	2011	Rice, soya, sugar and water	HMDE	DPASV	0.01	0.2–30	0.999	2.1	[26]
Pb ²⁺					0.017	0.5–70	0.999	2.55	
Cd ²⁺	2011	–	HMDE	DPASV	0.2	–	0.9989	<5	[27]
Pb ²⁺		–			0.07	–	0.9965		
Cd ²⁺	2010	Tap river, and geothermal water	SPE	FAAS ^b	0.38	1.26–22	0.9973	3.2	[28]
Cd ²⁺	2009	Tap river, sea and waste water	SPE	FAAS	0.2	1.0–20	0.9971	4.7	[29]
Pb ²⁺					3.2	10–300	0.9987	5.1	
Cd ²⁺	2009	Tap river, sea and waste water	USAEME	FAAS	0.91	10–600	–	1.62–2.65	[30]
Cd ²⁺		Tap river, and waste water	HF-GE	DPV	0.61	2–13000	0.9986	<5	Present work
Pb ²⁺					0.19	0.61–6500	0.9976		

^a Bi–SbFE^a: Bismuth–antimony film electrode, HF-SPME: hollow fiber solid phase microextraction, HMDE: hanging mercury drop electrode, USAEME: ultrasound-assisted emulsification–microextraction. ^bSWASV: square wave anodic stripping voltammetry, FAAS: flame atomic absorption spectrometry.

The relative standard deviations (RSD) were below of 5% (4.6%, $n=5$, $C_{\text{Cd}}=300 \text{ ng mL}^{-1}$ and 2.3%, $n=5$, $C_{\text{Pb}}=150 \text{ ng mL}^{-1}$).

It clearly shows that the proposed method of this study has good sensitivity and precision with a wide dynamic linear range.

3.4. Real samples analysis

The stated technique was applied for the determination of Cd(II) and Pb (II) in water samples. Well waters, mineral waters and tap waters were collected from the local points around Mashhad, Iran and wastewaters were collected from the industrial region of Mashhad, Iran. All of the samples were filtered before use. Some of the water samples lacked the analytes and were thus spiked with the Cd(II) and Pb (II) ions.

The relative recovery studies were performed in triplicate by spiking real water samples at a concentration level of 0.3 and $0.015 \mu\text{g mL}^{-1}$, before extraction. Simultaneous separation, pre-concentration and determination were conducted by diluting the real water samples in the supporting electrolyte. The diluted samples were then analyzed by spiking with appropriate concentrations of standard metal ion solutions. Each electrochemical measurement was carried out in triplicates.

To demonstrate the potential of this method as a viable extraction technique for real water samples, the standard solutions of cations were spiked into real samples. The relative recovery of real waters was determined as the ratio of the concentration in the real water and distilled water samples spiked at the same concentration level. The results are shown in Table 9 and Fig. 5.

4. Conclusions

This paper presented the results obtained for electrochemical DPV analysis of Cd(II) and Pb (II) ions using in-house fabricated electrode (HF-GE). The three-electrode configuration system coupled with differential pulse voltammetry has provided a means of a relatively inexpensive on-site sensor for trace levels of lead and cadmium. Detection of these metals was carried out using the optimized procedures developed for measurements in this work. With the optimized working conditions, the results indicated that the HF-GE electrochemical sensors were sensitive and reproducible enough for the DPV determination of cadmium and lead in the parts per billion ranges. The linear concentration range obtainable with HF-GE/DPV was wide.

For the environmental samples, the usefulness of DPV coupled to HF-GE for the determination of cadmium and lead in real water samples was evaluated. Overall, the results showed that the developed HF-GE electrochemical sensors were capable of measuring the analytes in different aqueous matrices.

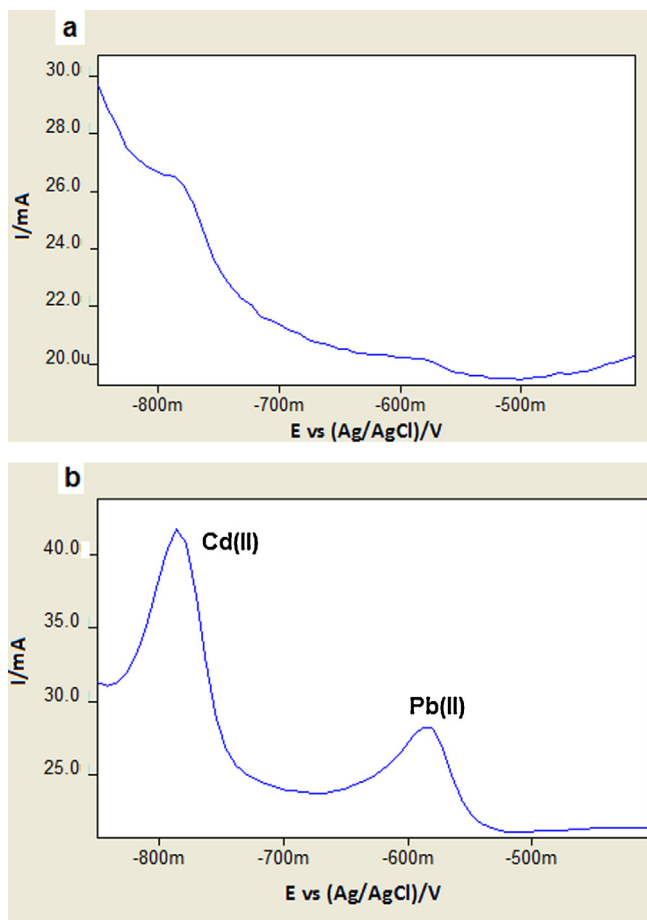


Fig. 5. HF-GE/DPV of river water, Mashhad, Iran: a) before spike and, b) spiked with 15.0 ng mL^{-1} Pb(II) and 30.0 ng mL^{-1} Cd(II).

The enhanced sorbent capacity was originated from the properties of the nanomagnetite, including small particle size, and homogeneous dispersion of the nanosorbent within the ionic liquid background. The above method also had the advantage of the strong interaction between analyte and sorbent.

Polypropylene wall pores are the channels which the analytes molecules and the nanosorbent were in contact with each other. Meanwhile, the pores can cause a kind of dimensional selectivity to the analyte molecules. Flexibility, simplicity, disposable nature of the device that eliminates the possibility of sample carry over, and high efficiency are among the advantages of this method.

The results demonstrated that the HF-GE/DPV can provide one-step simultaneous purification, pre-concentration, extraction, back-extraction and determination of electroactive analytes such as metal ions present in the feed and the advantage over conventional SPME coatings that often do not allow such effective extraction of polar analyte from the same sample.

Furthermore, allowing easy use of all types of nanoparticles, nanocomposites and ability to manipulate the structure of nanosorbents, give us the opportunity to selective and specific assay in a wide range of electroactive analytes. Despite the lack of using modern and expensive instruments, the results of this method are comparable. A review of selected methods which used in the determination of Cd(II) and Pb(II) in real samples is shown in Table 10.

Acknowledgment

The authors wish to thanks Payame Noor University for supporting of this research.

References

- [1] M.B. Arain, T.G. Kazi, M.K. Jamali, H.I. Afridi, N. Jalbani, J.A. Baig, Speciation of heavy metals in sediment by conventional, ultrasound and microwave assisted single extraction methods: a comparison with modified sequential extraction procedure, *J. Hazard. Mater.* 154 (2008) 998.
- [2] M.K. Jamali, T.G. Kazi, M.B. Arain, H.I. Afridi, N. Jalbani, A.R. Memon, Heavy Metal Contents of Vegetables Grown in Soil Irrigated with Mixtures of Wastewater and Sewage Sludge in Pakistan, using Ultrasonic Assisted Pseudo-digestion, *J. Agron. Crop. Sci.* 193 (2007) 218.
- [3] M. Karve, R.V. Rajgor, Solid phase extraction of lead on octadecyl bonded silica membrane disk modified with Cyanex302 and determination by flame atomic absorption spectrometry, *J. Hazard. Mater.* 141 (2007) 607.
- [4] B. Volesky, *Biosorption of heavy metals*, First ed., CRC Press, Boca Raton, FL, 1990.
- [5] S.L.C. Ferreira, J.B. Andrade, Review of procedures involving separation and preconcentration for the determination of cadmium using spectrometric techniques, *J. Hazard. Mater.* 145 (2007) 358.
- [6] E. Espada-Bellido, M.D. Galindo-Riano, M. Garcia-Vargas, Sensitive adsorptive stripping voltammetric method for determination of lead in water using multivariate analysis for optimization, *J. Hazard Mater.* 166 (2009) 1326.
- [7] J.-E. Belgaid, Release of heavy metals from Tunisian traditional earthenware, *Food Chem. Toxicol.* 41 (2003) 95.
- [8] E. Nagles, V. Arancibia, R. Ríos, Determination of lead and cadmium in the presence of quercetin – 5' – sulfonic acid by adsorptive stripping voltammetry with a hanging mercury drop electrode and a nafion?coated mercury film electrode, *Int. J. Electrochem. Sci.* (2012) 74545.
- [9] C.R. Teixeira-Tarley, V. Silva- Santos, B.E.L. d- Baêta, A.C. Pereira, L.T. Kubota, Simultaneous determination of zinc, cadmium and lead in environmental water samples by potentiometric stripping analysis (PSA) using multiwalled carbon nanotube electrode, *J. Hazard Mater.* 169 (2009) 256.
- [10] L. Hosseinzadeh, S. Abassi, Adsorptive Cathodic Stripping Voltammetry Determination of Ultra Trace of Lead in Different Real Samples, *Anal. Lett.* 40 (2007) 2693.
- [11] F. Ricci, A. Amine, G. Palleschi, D. Moscone, Prussian Blue based screen printed biosensors with improved characteristics of long-term lifetime and pH stability, *Biosens. Bioelectron* 18 (2003) 165.
- [12] M.-K. Hsieh, H. Chen, J.-L. Chang, W.-S. She, C.-C. Chou, Electrochemical detection of zeranol and zearalenone metabolic analogs in meats and grains by screen-plated carbon-plated disposable electrodes, *Food Nutr.Sci.* 4 (2013) 31. <http://www.zimmerusa.com/electrodes.html>.
- [13] E.O. Otu, J. Pawliszyn, Solid phase micro-extraction of metal ions, *Microchim. Acta* 112 (1993) 41.
- [14] J. Wu, W.M. Mullett, J. Pawliszyn, Electrochemically controlled solid-phase microextraction based on conductive polypyrrole films, *Anal. Chem.* 74 (2002) 4855.
- [15] Z. Es'haghia, M. Ahmadi-Golsefidi, A. Saify, A.A. Tanha, Z. Rezaeifar, Z. Alian-Nezhadi, Carbon nanotube reinforced hollow fiber solid/liquid phase micro-extraction: A novel extraction technique for the measurement of caffeic acid in *Echinacea purpurea* herbal extracts combined with high-performance liquid chromatography, *J. Chromatogr. A* 1217 (2010) 2768.
- [16] Z. Es'haghi, M. Ahmadi-Kalateh Khooni, T. Heidari, Determination of brilliant green from fish pond water using carbon nanotube assisted pseudo-stir bar solid/liquid micro- extraction combined with UV?Vis spectroscopy?diode array detection, *Spectrochim. Acta, Part A* 79 (2011) 603.
- [17] G. Gu, H. Jia, H. Li, B.J. Teppen, S.a. Boyd: Synthesis of highly reactive subnanosized zero-valent iron using smectite clay templates, *Environ. Sci. Technol.* 44 (2010) 4258–4263.
- [18] C.M. Cirtiu, T. Raychoudhury, S. Ghoshal, A. Moores, Systematic comparison of the size, surface characteristics and colloidal stability of zero valent iron nanoparticles pre-and post-grafted with common polymers, *Coll. Surf. A Coll. Surf. A* 390 (2011) 95.
- [19] Y. Cong, G. Wang, M. Xiong, Y. Huang, D. Zh Hong, Wang, J. Li, L. Li, A Facile Interfacial Reaction Route To Prepare Magnetic Hollow Spheres with Tunable Shell Thickness, *Langmuir* 24 (2008) 6624.
- [20] J.A. Lopez, F. González, F.A. Bonilla, G. Zambrano, M.E. Gómez, Synthesis and characterization of Fe₃O₄ magnetic nanofluid, *Rev. Latin Am. Metal. Mat.* 30 (2010) 60.
- [21] W.J. Yi, Y. Li, G. Ran, H. QunLuo, N.B. Li, Determination of cadmium(II) by square wave anodic stripping voltammetry using bismuth?antimony film electrode, *Sens. Actuat. B* 166 (2012) 544.
- [22] B. Ninwonga, S. Chuanuwatanakula, O. Chailapakula, W. Dungchai, S. Motomizu, On-line preconcentration and determination of lead and cadmium by sequential injection/anodic stripping voltammetry, *Talanta* 96 (2012) 75.
- [23] Z. Es'haghi, M. Khalili, A. Khazaeifar, G.H. Rounaghi, Simultaneous extraction and determination of lead, cadmium and copper in rice samples by a new preconcentration technique: Hollow fiber solid phase microextraction combined with differential pulse anodic stripping voltammetry, *Electrochi. Acta* 56 (2011) 3139.
- [24] S. Abbasi, A. Bahiraei, F. Abbasi, A highly sensitive method for simultaneous determination of ultra trace levels of copper and cadmium in food and water samples with luminal as a chelating agent by adsorptive stripping voltammetry, *Food Chem.* 129 (2011) 1274.
- [25] S. Abbasi, K. Khodarahmiyan, F. Abbasi, Simultaneous determination of ultra trace amounts of lead and cadmium in food samples by adsorptive stripping voltammetry, *Food Chem.* 128 (2011) 254.
- [26] J.A. Rodrigues, C.M. Rodrigues, P.J. Almeida, I.M. Valente, L.M. Goncalves, R.G. Compton, A.A. Barros, Increased sensitivity of anodic stripping voltammetry at the hanging mercury drop electrode by ultracathodic deposition, *Anal. Chim. Acta* 701 (2014) 152.
- [27] H. Ciftci, Separation and solid phase extraction method for the determination of cadmium in environmental samples, *Desalination* 263 (2010) 18.
- [28] H. Parham, N. Pourreza, N. Rahbar, Solid phase extraction of lead and cadmium using solid sulfur as a new metal extractor prior to determination by flame atomic absorption spectrometry, *J. Hazard Mater.* 163 (2009) 588.
- [29] J.J. Ma, X. Du, J.W. Zhang, J.C. Li, L.Z. Wang, Ultrasound-assisted emulsification-microextraction combined with flame atomic absorption spectrometry for determination of trace cadmium in water samples, *Talanta* 80 (2009) 980.